Investigation of Wave Forces on Fixed Monopile Foundation of Offshore Wind Turbine

Hassan Mohammed Alwan **Israa Yheaa Dawood** **Sajjad Jwad Kadhim**

[1,2,3]*Mechanical Engineering Department, University of Technology, Baghdad-Iraq*

Keffaat@mail.ru Israayheaa@yahoo.com zzaa8899@gmail.com

Submission date:- 29/12/2019	Acceptance date:- 8/9/2020	Publication date:- 20/10/2020

Abstract

The calculation of design loads on offshore wind turbine structures is a complex process. So, this thesis is performed to study and investigate the influence of environmental conditions on hydrodynamic loading acting on foundations of fixed offshore wind turbine. For this purpose, (5-MW) NREL monopile foundation was chosen. The foundation of wind turbine was tested at the intermediate water region with water depth (25m). The dimensions of the foundation and water depth beside wave properties were modelling by using Froude relationships with scale ratio (1:100). Two-dimensional (regular) and non-breaking waves were tested. Morison equation for non-diffracting case was used and programmed by using (C++) language to compute the wave forces. This equation delivers the sum of drag and inertia force. Inertia force is proportional to acceleration wave particle while the drag force is related with the velocity particle. The two coefficients of equation (C_M,C_D), inertia and drag respectively are estimated according to Det Norske Veritas (DNV) standard. A classical linearized wave theory has been developed by Airy based in this paper, this theory has been used to estimate the kinematics properties (velocities and accelerations) of the wave particles. Numerically, the wave will simulate by using **(**AQWA) solver in (ANSYS-19.0) workbench. It was shown that the wave forces is related with the height and frequency of wave, it is increase when one or both of wave height and wave frequency increase.

Keywords- Airy wave theory, Monopile foundation, Offshore wind turbine, ANSYS AQWA, Drag force, Inertia force.

1-Introduction:

The phenomenon of climate change resulting from high concentration of (Co_2) in atmosphere of the earth has become one of the major problems facing the world. Therefore, researchers and specialists worked for decades to find the solution to avoid or minimize the effects of these risks. To overcome these constraints, the harvest of wind energy through the use of large wind turbines is likely to play a major role, especially as the political and industrial interests have begun to focus on the offshore wind energy production. Offshore wind turbines (OWT) represent an exciting new area for the industry, largely due to the higher wind speeds available and economies of scale allow for the installation of larger-scale wind turbines offshore [1]. The analysis, design and construction of offshore structure are arguably one of the most demanding sets of tasks faced by the engineering profession. Over and above the usual conditions and situations met by land-based structures, offshore structures have the added complication of being placed in a seas environment where hydrodynamic interaction effects and dynamic response become major considerations in their design. [2]

Jeong [3] investigated the effects of sea levels and wave conditions on the wave force. Three sea levels and eight wave conditions for the three models type of the offshore support structure (monopile, gravity-based structure, and jacket structure) were considered. It was found that the larger diameter of support structure within the range of this study, the larger the diffraction effect is, and the increase in wave force due to shoaling is suppressed. Mendes, et al. [4] have introduced a theoretical predictions of the environmental loading induced upon an offshore structure. The methodology that has been used in calculation of hydrodynamic loading was based on Morison formula. Linear wave theory (Airy theory) was used to estimate water-particle kinematics. The model structure is a Four-legged tubular structure scaled-down with scale ratio (1:28) from a realistic offshore platform. It was noted that the hydrodynamic forces increased with wave height and with coupled influence of waves and current. At significant current velocities the overall loading is essentially dominated by drag, which may represent as much as (60%) increase in maximum horizontal force. Pradip Dip Roy [5] used a Small an amplitude linear wave theory on vertically circular thin plates under three positions: (a) a surface-piercing, (b) a submerged, (c) a bottom standing. Morison's equation is used to calculate wave force. Horizontal wave force and moment are obtained with respect to the wave amplitude at different incident angles of wave as well as with different depth of water and different wave period. Note that these forces and moments against wave amplitude are extremely high for small wave period. So, the force and moment in case (1) are maximum compared with (b) and (3) ant any amplitude of wave. Min-Su Park et al. [6] used ANSYS AQWA to evaluate the wave forces acting on the gravity base structure for (5MW) offshore wind turbine. The wave forces and panel pressure on the substructure are presented for various water depth. It was found that the total wave forces on gravity substructure gradually decreased as the water depth increases because the wave force is closely related to the wetted surface of substructure and the water particle velocity near free surface is largest. Masoomi, [7] the purpose of this thesis is to investigate the loadings on and motion of an offshore wind turbine. The (NREL-5 MW) offshore model wind turbine was chosen for this study. A wide range of waves with different amplitudes and frequencies were generated. The experiments were conducted within a water flume at the University of Toledo. All tests on the scale model platforms were conducted in a water flume, which consists of (45 cm deep × 30 cm wide × 250 cm long) water tank. Force measurements were done by using load cell sensor. A video camera was used to measure wave properties. Labview was used to collect and process the sensor's signals. It was shown, that the rise of the force in the (x) direction is due to waves impacting the surface of the platform. Yongjun Jian [8] in this study, an analytical solution for the diffraction of short crested incident wave on a large diameter circular cylinder was derived. The effect of currents on wave frequency, water run-up, and wave force on the cylinder profiles are investigated. It was shown that the wave loads exerted on a cylinder with currents would be larger compared to the wave loads exerted pure short-crested waves.

Yu-Hsien Lin [9] a hydrodynamic simulation of wave run-up heights and wave loads on three types of wind turbine foundations (monopile, gravity-based and tripod support structures) was conducted by using (RANS) solver. The results shown that the difference in the maximum run-up heights of these support structures is smaller for lower wave steepness than those for higher wave steepness. Also, it is shown that the difference in the wave loads of these foundations is larger for lower wave steepness than those for higher wave steepness. Bo Terp Paulsen [10] Two-dimensional irregular waves on a sloping bed and their impact on a bottom mounted circular cylinder is modeled by three different numerical methods. A linear, a fully nonlinear potential flow solver and a fully nonlinear Navier-Stokes/VOF solver was used for this purpose. The results are validated with laboratory experiments results. Large deviations was recorded for linear potential flow when compared with the experimental measurements. Fully nonlinear Navier-Stokes/VOF calculations are accurately predicting both the free surface elevation and the inline force. A good agreement was recorded between the nonlinear potential flow in two-dimensions and three-dimensional Navier-Stokes/VOF solver. For the steepest near breaking waves the inline force is more accurately captured by the Navier-Stokes/VOF solver due its ability to handle wave breaking. Ankit Aggarwal [11] introduced a simulations of regular and irregular wave with different properties interaction with a vertical cylinder are carried out using the open source Computational Fluid Dynamics (CFD). It was observed that the regular waves with higher steepness show a clear diffraction pattern around the cylinder. For the irregular waves, the diffraction pattern is less developed and random. Aliyu Baba [12] estimated hydrodynamic loads on fixed offshore structures (inclined and horizontal cylinder) for offshore platform. For the purpose of this study, linear (Airy) wave theory was used. The forces were estimated by using Morison equation. It was shown that the value of the force in the (x-direction) increases with change in sea state, while the value of the forces in the (z-direction) increase in an irregular pattern with change in sea states. Vorhoelter [13] this papers compares different approaches to determine the design forces and moments for the ultimate limit state for monopile structures for offshore wind turbines. Four different methods (volume of fluid method, boundary element method and the Morison formula) are compared to each other. For the calculation of forces and moments with the (BEM), method the potential solver panMARE of the (Institute for Fluid Mechanics and Ship Theory) of Hamburg University of Technology is used. Investigations have been performed for various wave heights, periods and model scales. It was shown that when the crest or the trough are at the center of the pile the resulting force and moment is close to zero. For the shear force, the experimental test gives the same results as the (BEM) computation. Noorzaei [14] described the analytical and numerical method to calculate wave and current forces on slender structural members (vertical cylinder). The cylinder will divided into (5, 10 and 15) elements. Two common wave theories have been conducted in this study, namely (Airy's linear theory) and (Stokes fifth order theory). For comparison purposes, the developed program were checked against a commercial software package called Structural Analysis Computer System (SACS). For Airy's wave theory, the average percentage error of the present study compared to (SACS) is (1.68%, 2.62%, and 2.80%). For stokes fifth order theory, average percentage difference of the present study compared to SACS is (1.96%, 2.62%, and 2.74%).

In present project, the resources required to implement the experiment on more than one type of foundations or even to generate different type of waves it not easy to provide. Therefore, this study will be limited to specific type of water waves which is regular waves. Another type (irregular waves) consider a combination of various regular wave frequencies, so this study can be useful to get a general idea about random waves.

2. Monopile foundation

Monopile foundations as shown in figure (1) is one of the simplest types of offshore wind turbine. It consists of a vertical tubular pile with a diameter in the range of (3-6 m). Steel is the most common material used in the construction of the monopile foundations. Pile foundation is generally used when the top layer consists of soft soil and when large horizontal loads are applied to the structure. The diameter of the foundation and the thickness of the steel is decided by the bottom substrate, the water depth, the weight of the turbine, the height of the tower and the load (weight stress) from the currents and waves. [15]

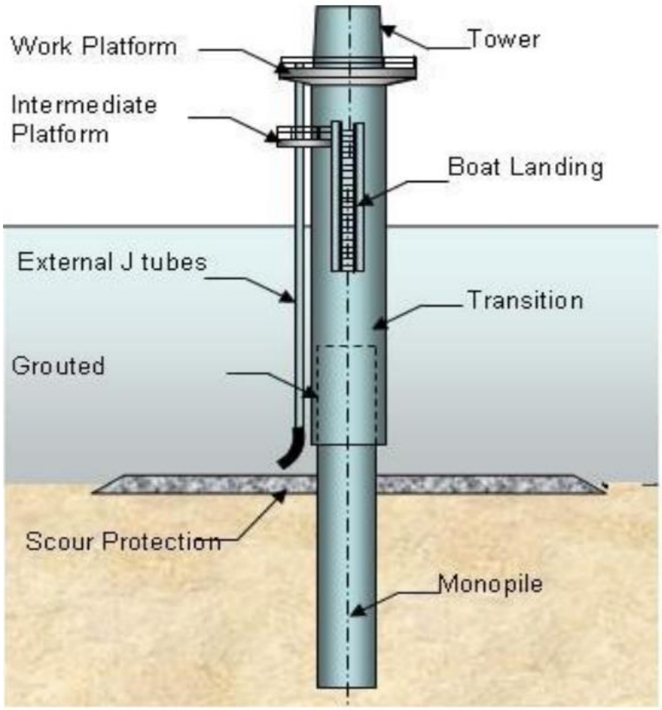

Figure (1): Monopile foundation

3. Model structure

The model structure has been scaled down from a realistic monopile foundation. The total height of foundation is (30m), of which (25m) underwater. The external diameter is (6m) and (90mm) wall thickness. All dimensions scaled down by using Froude laws with scale ratio (1:100).

4. Froude laws

Froude scaling was used for establishing scaling factors between the model and the full scale foundation. A geometric scaling ratio used for this scaling is first defined by:

$$\lambda_l = L_{FS}/L_{Md} \quad (1)$$

Here (FS) denotes full-scale and (Md) denotes model. The geometric scaling factor (λ_l=100) in test. A Froude number is defined next by:

$$Fr = U/\sqrt{g\,L} \quad (2)$$

Where (U) is a characteristic velocity and (L) is a corresponding characteristic length. The characteristic velocity in the model, U_{Md} is then calculated by matching Fr in the model and full-scale ($Fr_{Md} = Fr_{Fs}$). Thus

$$U_{Fs} = U_{Md}\sqrt{L_{Fs}}/L_{Md} \quad (3)$$

Then, the characteristic velocity ratio between model and full-scale is given by:

$$U_{Fs} = U_{Md} \times \sqrt{\lambda_l} \quad (4)$$

The scale ratio for any important physical parameter in this problem can then be determined in a similar fashion. Table (2) describes the scaling of common parameters for the wind turbine foundation and also for wave properties. [15]

Table (1): scale ratio for common dimension and properties

$\lambda = Fs/Md$			
Variable	Dimensions	Units	Scale ratio
Wave height Wave length Foundation diameter Water depth	L	m	λ
Force	$M \times L/T^2$	$kg \times m/s^2$	${\lambda_l}^3$
Wave Period	T	s	$\sqrt{\lambda_l}$
Velocity	L / T	m/s	$\sqrt{\lambda_l}$

5. Airy theory

In order to calculate the hydrodynamic forces acting on the members of an offshore structure, it is required first to describe the sea state as occurring in nature which determines the wave surface profile and then the characteristics of the water wave particles hitting the structure. For this purpose, a relatively simple theory of wave motion, known as (Airy's linear theory) was given by (G.B. Airy in 1842). This theory is most accurate for low amplitude waves in deep water, less accurate for predicting wave behavior in shallow water, the most commonly used wave theory because it is the least mathematically complex one and does not take into account the effect of wave height in determining wave velocity. It is also assumed that the water waves are represented as two-dimensional plane and wave height is small in comparison with the wavelength ($H \ll \lambda$). [16]

The theory assumed that the waves are two dimensional in the (x-z) plane and that they propagate over a smooth horizontal bed in water of constant undisturbed path. The surface elevation of linear wave amplitude (a) at any instance of time (t) in the direction of travel of wave (x-direction) as shown in figure (2), is denoted $\eta(x,t)$ and is given by:

$$\eta(x,t) = a\,cos(\omega t - kx) \tag{5}$$

Where,

λ: Wavelength

T: Wave period

W: the wave frequency = $2\pi/T$

K: wave number = $2\pi/\lambda$

The vertical velocity w (z) and horizontal velocity u(x) in Airy theory at position (z) (see figure 2) are measured from mean water level in depth water (d) are given by

$$u = \omega a \frac{\cosh k(z+d)}{\sinh kd} \sin(\omega t - kx) \tag{6}$$

$$w = \omega a \frac{\sinh k(z+d)}{\sinh kd} \cos(\omega t - kx) \tag{7}$$

The horizontal acceleration $\dot{u}(x)$ is given by derivative equation (2)

$$\dot{u} = \omega^2 a \frac{\cosh k(z+d)}{\sinh kd} \cos(\omega t - kx) \tag{8}$$

While the vertical acceleration $\dot{w}(z)$ is given by derivative equation (3)

$$\dot{w} = -\omega^2 a \frac{\sinh k(z+d)}{\sinh kd} \sin(\omega t \ - kx) \tag{9}$$

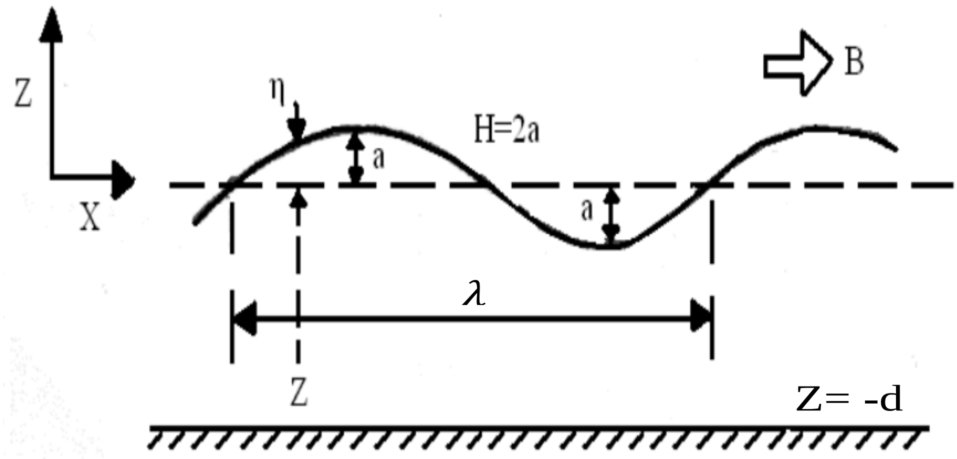

Figure (2): Progressive water wave

All above equations are applied for small water depth region when the condition (d/ λ) is less than (0.5).

For deep water region, the ratio (d/ λ) should be more than (0.5). So, the equations from (2) to (5) will be

$$u= \omega a e^{kz} \sin(\omega t - kx) \tag{10}$$

$$w = \omega a e^{kz} \cos(\omega t - kx) \tag{11}$$

$$\dot{u} = \omega^2 a e^{kz} \cos(\omega t - kx) \tag{12}$$

$$\dot{w} = -\omega^2 a e^{kz} \sin(\omega t - kx) \tag{13}$$

6. Morison equation

Wave force on cylindrical elements are of considerable interest in the design of offshore facilities. Morison et al. (1950) proposed a simple equation expressing the total wave force as the sum of drag and inertia force. Inertia force is proportional to acceleration wave particle while the drag force is related with the velocity particle. This formula is strictly limited for use with slender structural element characterized by $\left(\frac{\lambda}{D} < 0.2\right)$ [16]. The general Morison formula is given by:

$$F = C_M \rho \frac{\pi}{4} D^2 \dot{u}(t) + C_D \frac{1}{2} \rho D u^2 \tag{14}$$

The inertia force on a fixed cylinder is the sum of two terms

Froude-Krilov force is given by:

$$F_{X1}(t) = \rho \pi R^2 . \dot{u}(t)$$

And force due to added mass which is given by:

$$F_{X2}(t) = \rho \pi R^2 . \dot{u}(t) \tag{15}$$

$$\therefore F_I(t) = F_{x1}(t) + F_{x2}(t) \tag{16}$$

$$= 2. \pi R^2 \rho . \dot{u}(t) \tag{17}$$

The theoretical value of (2), is usually replaced by an experimental coefficient (CM). It is made up of (1) from (Fx1) (the ambient pressure field) and (1) from (Fx2), the flow disturbance caused by the cylinder.

$$\therefore F_I(t) = C_M . \pi R^2 \rho . \dot{u}(t) \tag{18}$$

The other part of Morison equation is drag force which defined the resultant fluid force acting on a body in a flow of constant velocity, or equivalently, the resistance experienced by a body moving with constant velocity through a still fluid. The drag force can be specified as,

$$F_D(t) = C_D \frac{1}{2} D \rho u^2 \tag{19}$$

7. Coefficients of Morison equation

They depend, in general, on the flow properties surface roughness, Reynolds number (Re) and non-dimensional parameter keulegan-carpenter (KC) where,

$$\mathrm{KC} = 2\pi\, a/D \qquad (20)$$

The Keulegan-Carpenter number describes the contribution of the drag force to the total force, where the inertia forces dominate at the low value of the Keulegan-Carpenter number (less than 3) and the drag forces dominate at the Keulegan-Carpenter number of (more than 40).

The coefficients can be determined based on experimental data. Hundreds of researchers had conducted laboratory tests to determine (CD) and (CM). The data which obtained from Det Norske Veritas [DNV] or the American Petroleum Institute (API) consider the most widely accepted. Figure (3) illustrated the values of (CM, CD) for both smooth and roughness cylinder according to (DNV). [16]

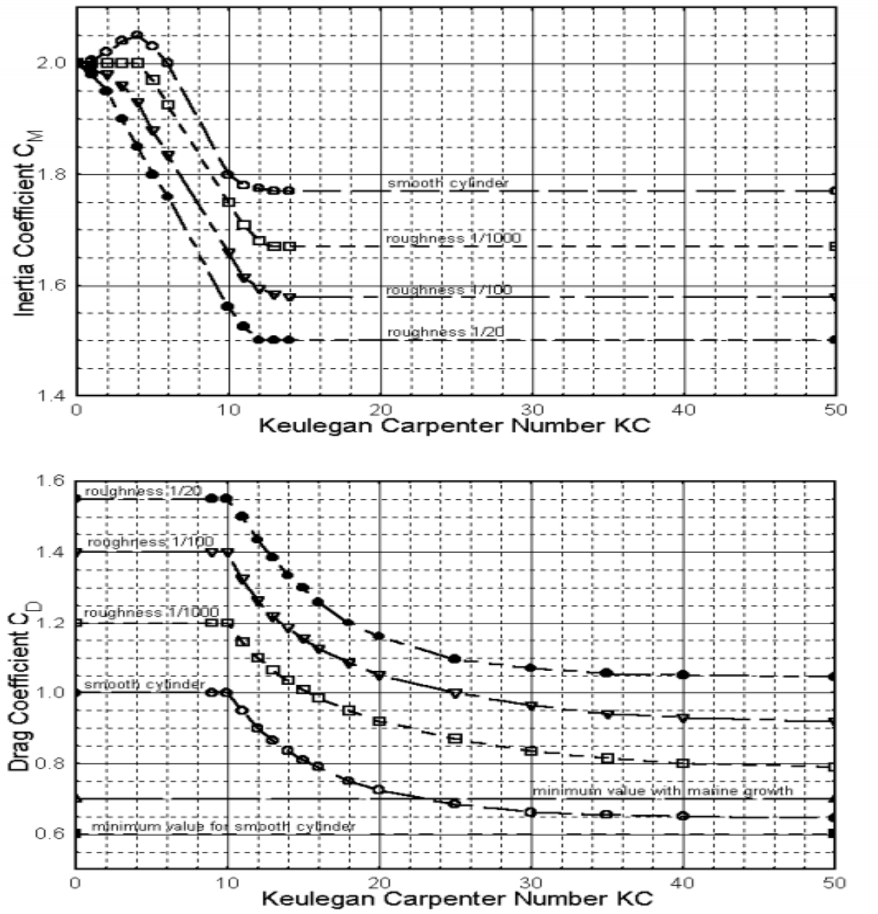

Figure (3): Drag and Inertia coefficients values according to (DNV).

8. Theoretical calculation

Figure (5) refers to the flowchart of calculation procedure in this study, which was implemented by using (C++) language to estimate kinematics properties of waves and hydrodynamic loads effect on the foundation of wind turbine. The geometry of foundation as shown in figure (4) will be known with number of elements and each element define by two main nodes. The submerged part of cylinder will be (25m), it will divide into (6) elements with (7) nodes. The input file of the program will include, wave properties, number of elements and Cartesian coordinate of nodes. The calculation are done for every element, number of nodes will generate for each element between two main nodes. The acceleration and velocity components calculated of time series on each node.

Inertia force, drag force and total force will determine by applied Morison equation at each node. The mean value of forces [(F1(x), F2(x), F3(x), F4(x), F5(x), F6(x)] for all elements and total load (summation of all forces on the foundation) are calculated at each time step.

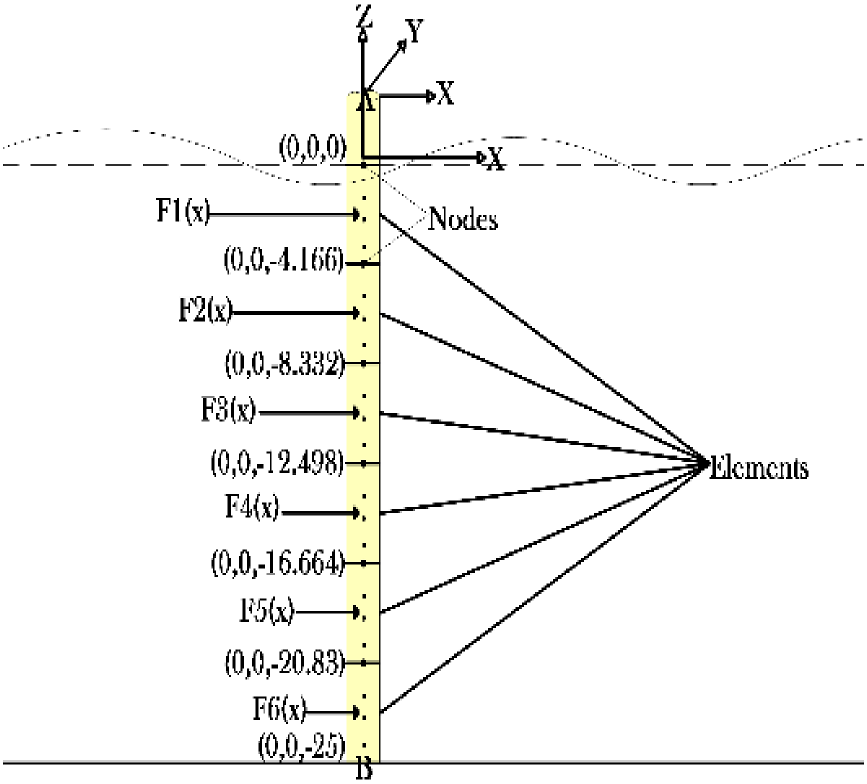

Figure (4): The foundation with effect force.

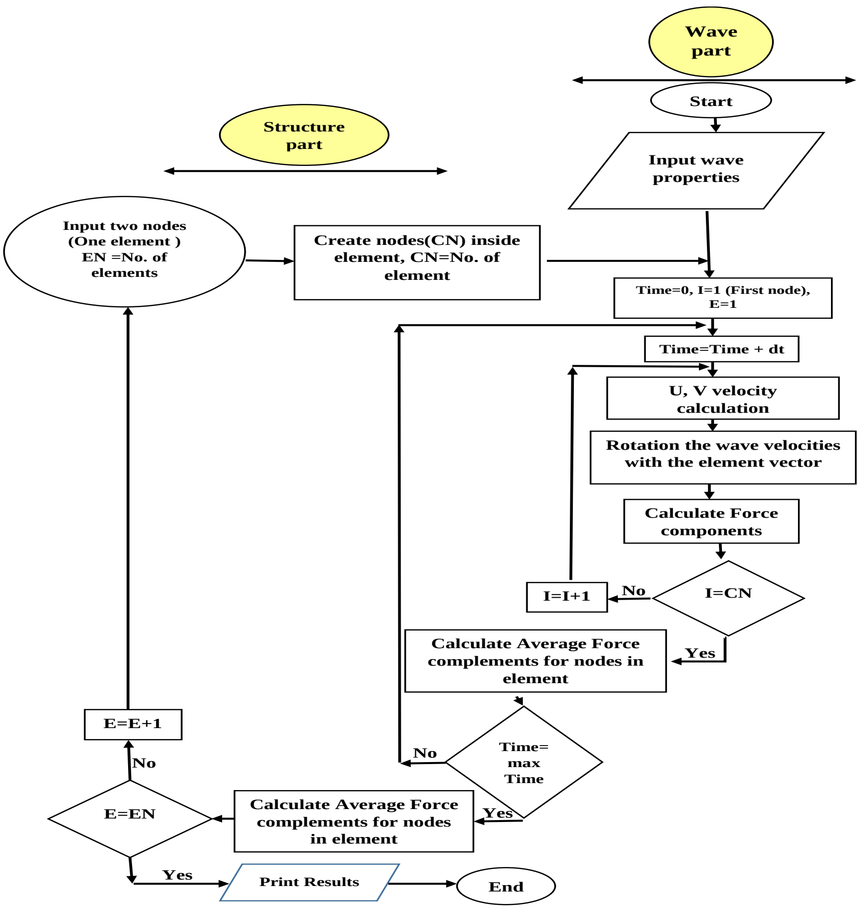

Figure (5): Flowchart explain the steps to compute Morison's force.

9. Numerical calculation

ANSYS AQWA provides an engineering toolset for the investigation of the effects of waves on floating and fixed offshore and marine structures. AQWA can simulate linearized hydrodynamic fluid wave loading on floating or fixed rigid bodies. This is accomplished by employing three-dimensional radiation/diffraction theory and/or Morison's equation in regular waves in the frequency domain. Morison element forces relate to all non-panel elements that can attract wave and current loading. In AQWA, cylindrical tube and disc elements can be defined. The major technique used in this solver for discretization is boundary element method (BEM). It is probably the most popular method used for numerical discretization in ANSYS AQWA. The main differences between Finite Element Method (FEM) and Boundary Element Method (BEM) is the way the domain is discretized. In both of them the problem domain is divided into finite elements. The (FEM) requires a discretization of entire domain, preserving the dimensional order of the problem. The (BEM) operates on the discretization of the boundaries, which reduces the terms of the problem by one dimension, also the time analysis required to simulate waves and compute forces is less compared with (FEM). [17 18]

10. AQWA Simulation Steps:

ANSYS AQWA solver includes two parts [17], see figure (6):

1-Hydrodynamic diffraction: provides an integrated environment for developing the primary hydrodynamic parameters required for undertaking complex motions and response analyses.

2-Hydrodynamic time response: provides dynamic analysis capabilities for undertaking global performance assessment of the structures in the time domain.

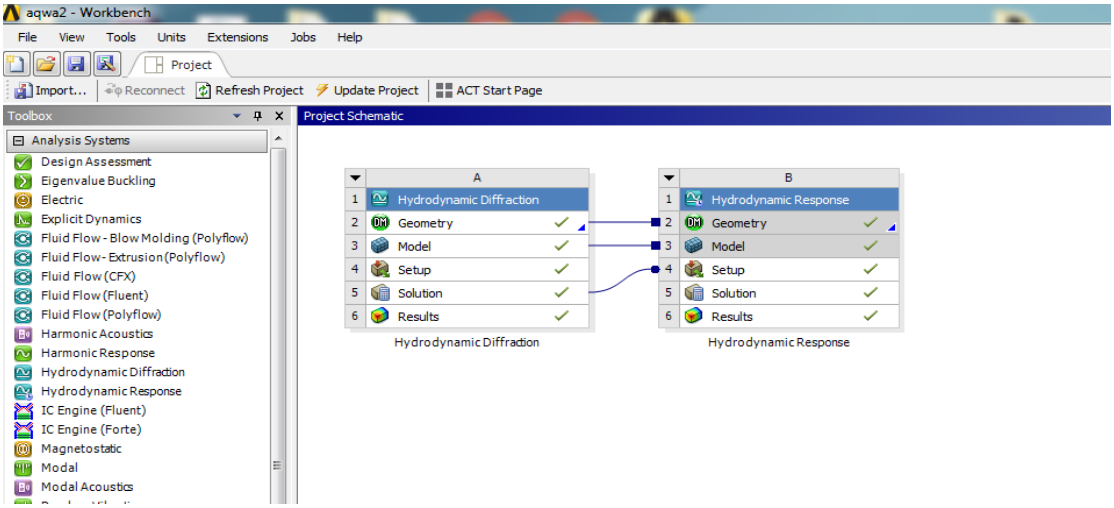

Figure (6): Modal analysis by using ANSYS program.

10.1 Create a Hydrodynamic diffraction analysis System:

This part will include the following steps:

1. Draw the sample (cylinder) inside ANSYS workbench.
2. Generate the geometry of the sample.
3. Choosing the dimensions of cylinder (height, diameter), also the cylinder has to be surface, so for this purpose should select "Thin/surface".
4. Structure's longitudinal axis must be on the Z axis, also the model has to be split at the water line as shown in figure (7). The whole height of the cylinder will be (30m), (5m) above water line and (25m) will be below.

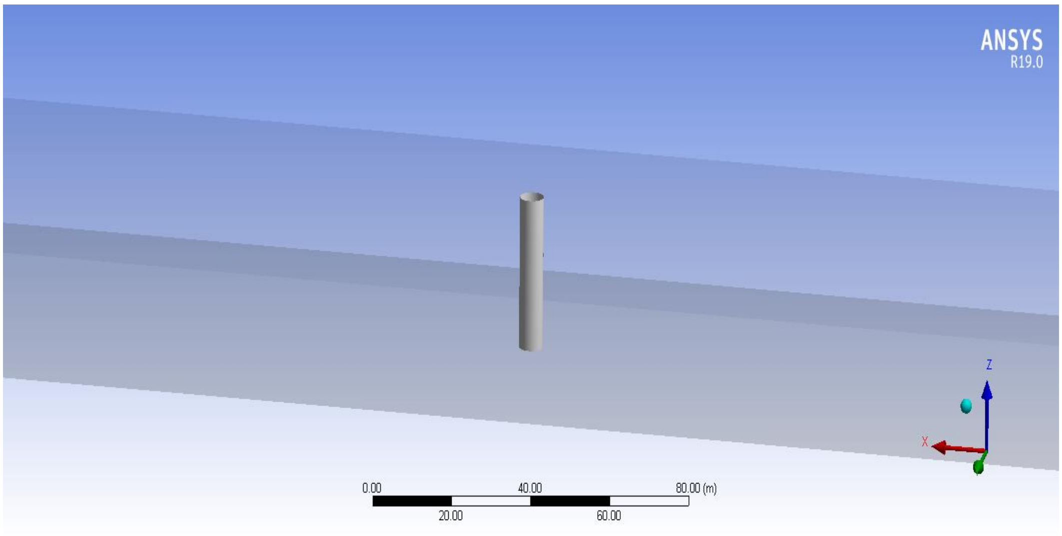

Figure (7): The Sample.

5. The depth of the sea can be defined. For this analysis it will be fixed to (25m). The size of the water will affect the display and will be (300m) for (X) and (100m) for (Y).
6. Also the mass properties of the cylinder must be included to make the result more accurate.

For this analysis, the mass properties will be:

Mass = 399313.8 kg

Density = 7850 kg/m^3

I_X= 1796912.1 kg.m^2

I_Y= I_Z= 30846991.05 kg.m^2

I_{YZ}= 29948535 kg.m^2

I_{XY}=I_{ZX}= 89845605 kg.m^2

6. To specify a range of frequencies, it is required to set the starting and ending frequency.

.Start frequency > 0.16 / (Water Depth) ^0.5.

.End frequency < 0.51 / (Max Element Size) ^0.5.

.End frequency > 1.1 Start Frequency.

For this analysis (start frequency= 0.04 HZ and end frequency = 0.667).

7. **Mesh:** Grid generation is the process of dividing the domain into small elements. There are several different types of grids, including hexahedral, tetrahedral, prisms, see figure (8). The mesh is based on the defeaturing tolerance and maximum element size parameters.

- **The Defeaturing Tolerance:** controls how small details are treated by the mesh. If the detail is smaller than this tolerance then a single element may span over it, otherwise the mesh size will be reduced in this area to ensure that the feature is meshed. The defeaturing tolerance cannot be greater than 0.6 × max element size.
- **Max Element Size:** controls the maximum size of the element that will be generated. In AQWA this is related to the maximum wave frequency that can be utilized in the diffraction analysis.

In this analysis, the maximum element size will be (0.5) and defeaturing tolerance will be (0.09).

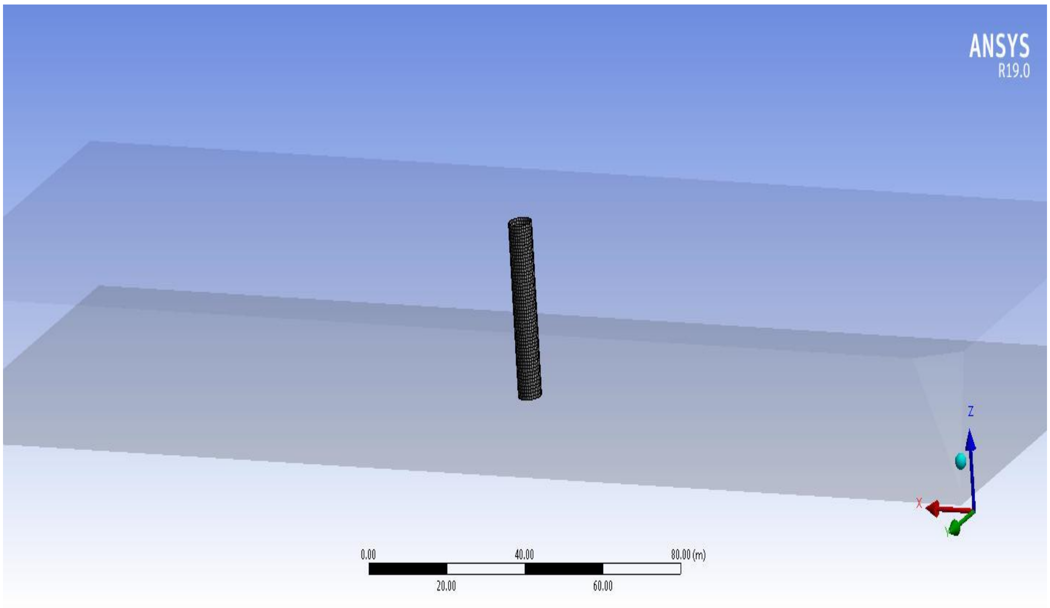

Figure (8): Generated mesh by ANSYS program.

8. Apply the boundary conditions including the support of the sample, since the case is only limited to regular waves, so the direction of the wave will be single direction as shown in figure (9).

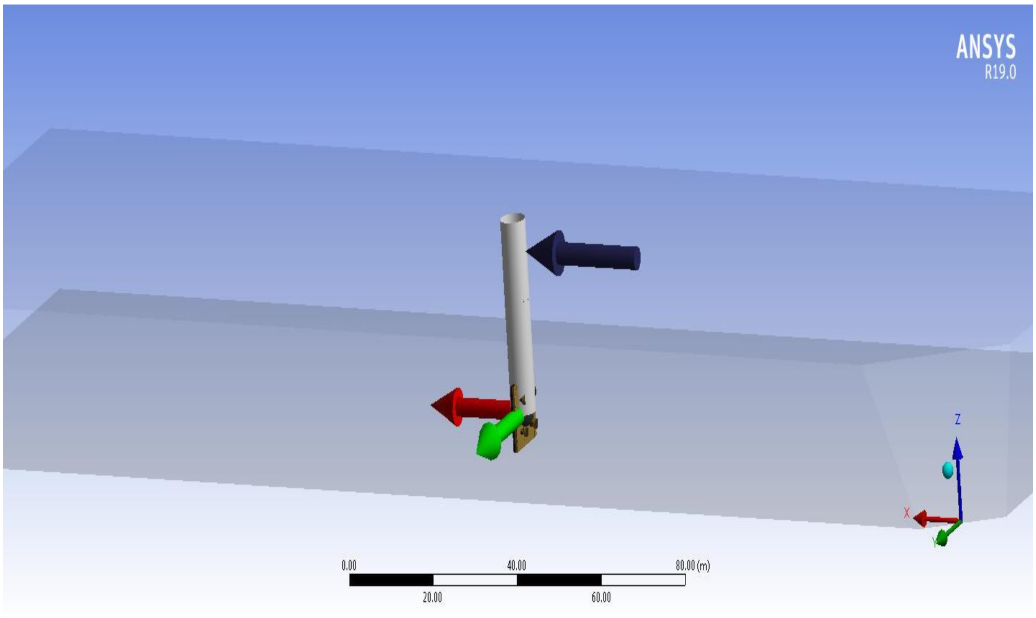

Figure (9): The direction of regular wave.

9- Choosing the wave frequency and amplitude, after that solving the model by using solve analysis.

<u>10.2 Hydrodynamic time response:</u>

The analysis settings in this section will include:

1- Choosing the type of wave (Regular or Irregular wave) and the wave theory, for this analysis it will be a regular wave and Airy's theory.

2- Entering frequency or period for the wave beside the amplitude. This period / frequency should be within the range of that in the Hydrodynamic Diffraction analysis.

3- Select the Start Time and Finish Time for the Time response simulation. Then choose Time Step or Number of Steps.

4- Solving the model and then calculate a time history of structure forces in (x-direction), see figure (10).

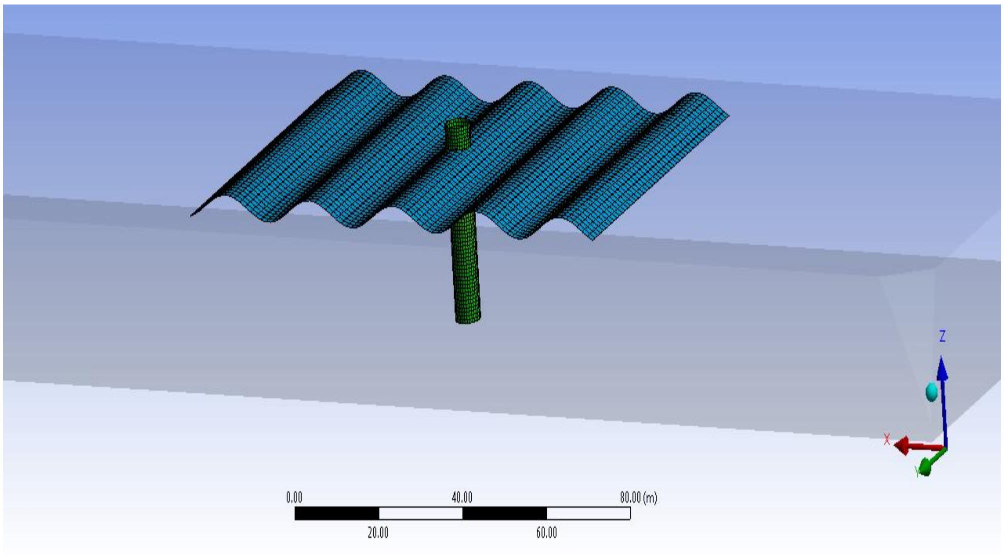

Figure (10): Simulation of waves.

11. Experimental setup

A rectangular wave flume with dimensions (3m length, 1m width and 63cm height) was built for the aim of this test. The flume will be filled with water. The height of water will be at (25cm). To generate waves, a piston type wavemaker was built for this purpose. This gate will move by using (AC) motor which connect with Ac drive to control the speed. A set of sacks will be filled with sawdust, this sacks will be putted in the other side of flume to reduce the effect of reflection waves.

The wave frequency will be estimated by using a nikon camera (3200). Select a specific point on the surface of flume glass, then record a video by the camera, slowing the video and then account the number of waves which will cross this point during (16s), after that the number of waves will divide on the duration of time, then will get the frequency. The wave height and length will be measured by using tape measure which drawn on the surface of flume glass.

Six load cell sensors placed on the submerged part of the cylinder was used to measure the wave frequency, the distance between these sensors will be equal to (4.1cm). When the waves reaches to the cylinder and hits the sensors which located near the water level as well as the others which placed at bottom also will be effected, these sensors will transduce the signals to the software (Lab-view) which will treated with it and after that the results will display on the computer, figure (11) clarify the test procedure of this study.

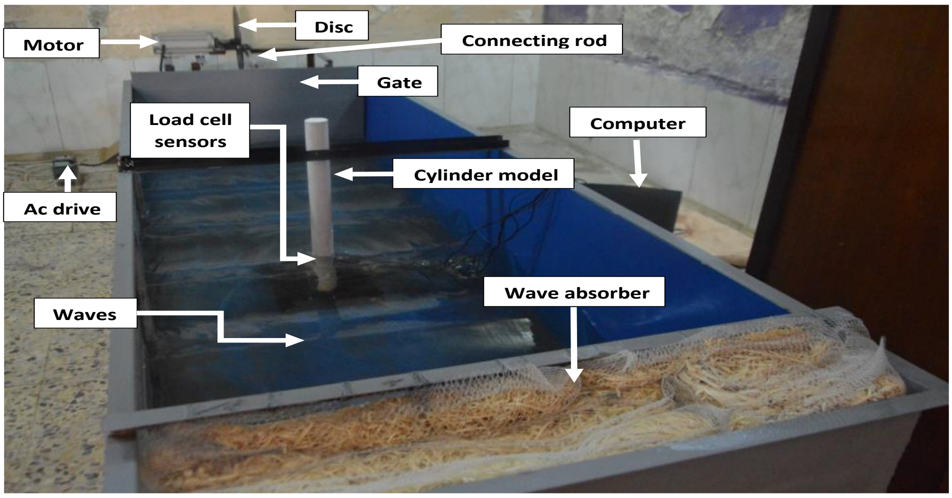

Figure (11): Test procedure.

12. Results and discussion

In this study, the characteristics of waves for all cases are generated by using inclined paddle-type wavemaker. The relationships between wave amplitude and paddle stroke are established for different inclinations of the paddle-type wavemaker, based on the boundary collocation method (BBM) as illustrated in Ref. [19]. Four cases for different wave properties as shown in figure (12) has been generated and tested in experimental part from this study. Change the gate angle, the gate frequency and the gate stroke helped to get these cases. The first and second case have the same wave frequency but the wave height is change to study the effect of increasing wave height on the wave force. Also, the second case has the same wave height with fourth case, but the frequency is change. Table (2) shows the normal wave properties and also the scaling wave properties.

Table (2): Wave properties for four cases.

No.	Normal wave properties				Scaling wave properties			
Wave properties	**H(m)**	**F(HZ)**	**T(S)**	**λ(m)**	**H(cm)**	**F(HZ)**	**T(S)**	**λ(cm)**
Case I	2.5	0.625	1.66	70	2.5	0.0625	16.6	70
Case II	4.25	0.625	1.66	70	4.25	0.0625	16.6	70
Case III	3.75	1.1	0.9	62.5	3.75	0.11	9	62.5
Case IV	4.25	1.18	0.84	51	4.25	0.18	8.4	51

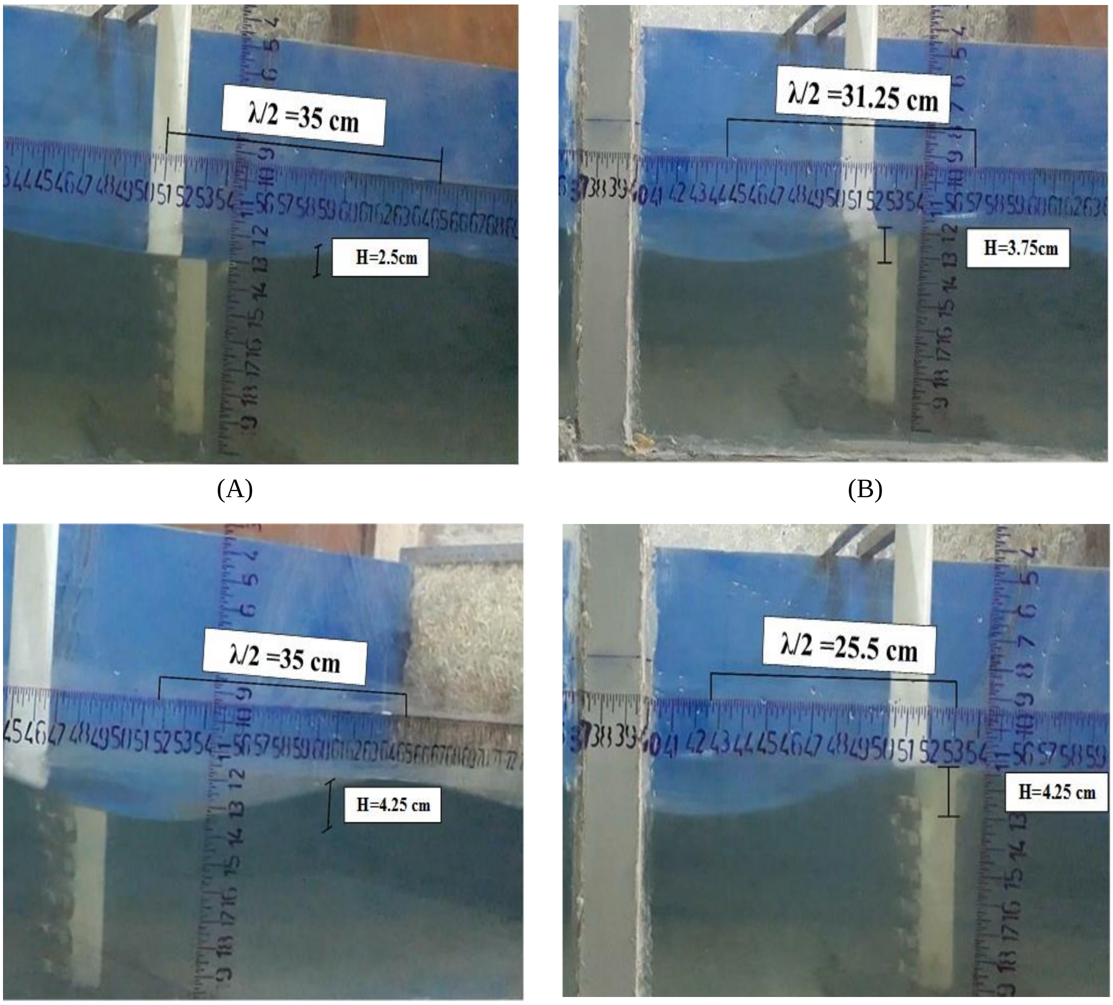

(A) (B)

(C) (D)

Figure (12): shows four cases (A, B, C and D) with different wave properties.

Regarding the first part, figure (12) present the time history of wave force for each element on the monopile foundation along the wave propagation direction (x-direction). it was shown that the hydrodynamic force is proportional to the water depth, it is found that the maximum value of the wave force at the surface of the water when (Z=0), and begins to decrease gradually until reach to the minimum value at the bottom of the foundation. In the first two cases (I and II) especially when the frequency of the particle is a little, it is noted that the maximum value of wave force for the first element is close for that value in last element (6), in contrast to the last two cases (III and IV), noticing that there is a big difference between these values, this is due to kinematics properties of wave particle which in turn will effect on wave forces. In intermediate water region and when the wave frequency is a little, the change in kinetics energy from the bottom of the sea to the sea surface will be a little because the probability of breaking waves which has a big role on kinematics properties at the surface of sea water in this region is very small.

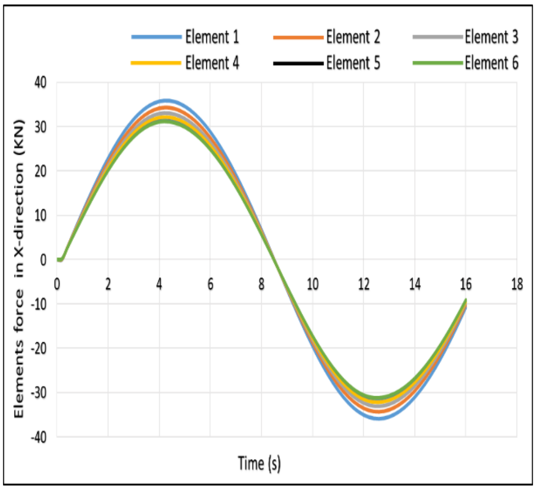

(A)

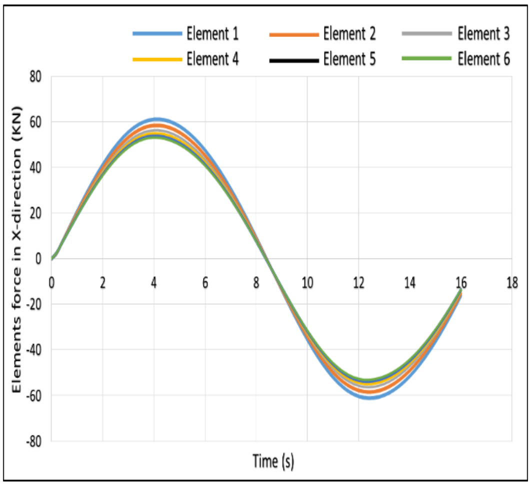

(B)

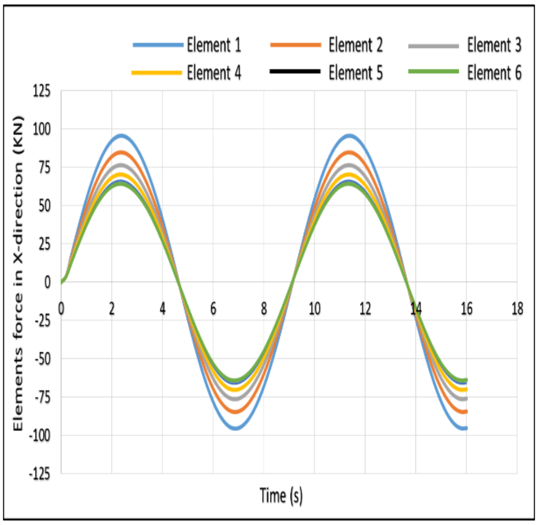

(C)

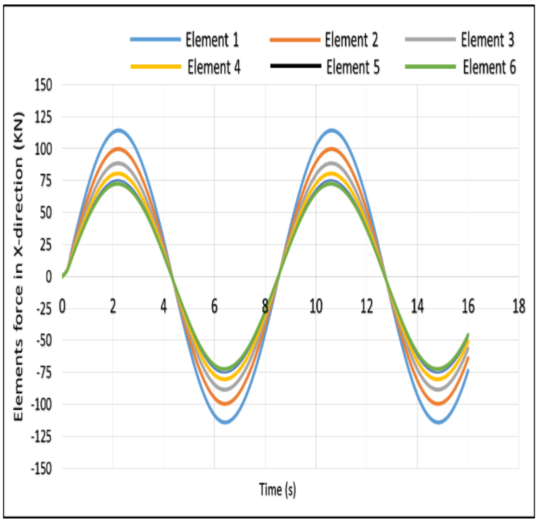

(D)

Figure (12): Elements force for four cases.

Figure (13) shows the wave forces are plotted against time, (16s) with time step (0.2) was selected as duration time for each case. The roughness of the cylinder was not taken into consideration when calculate the (KC) number.

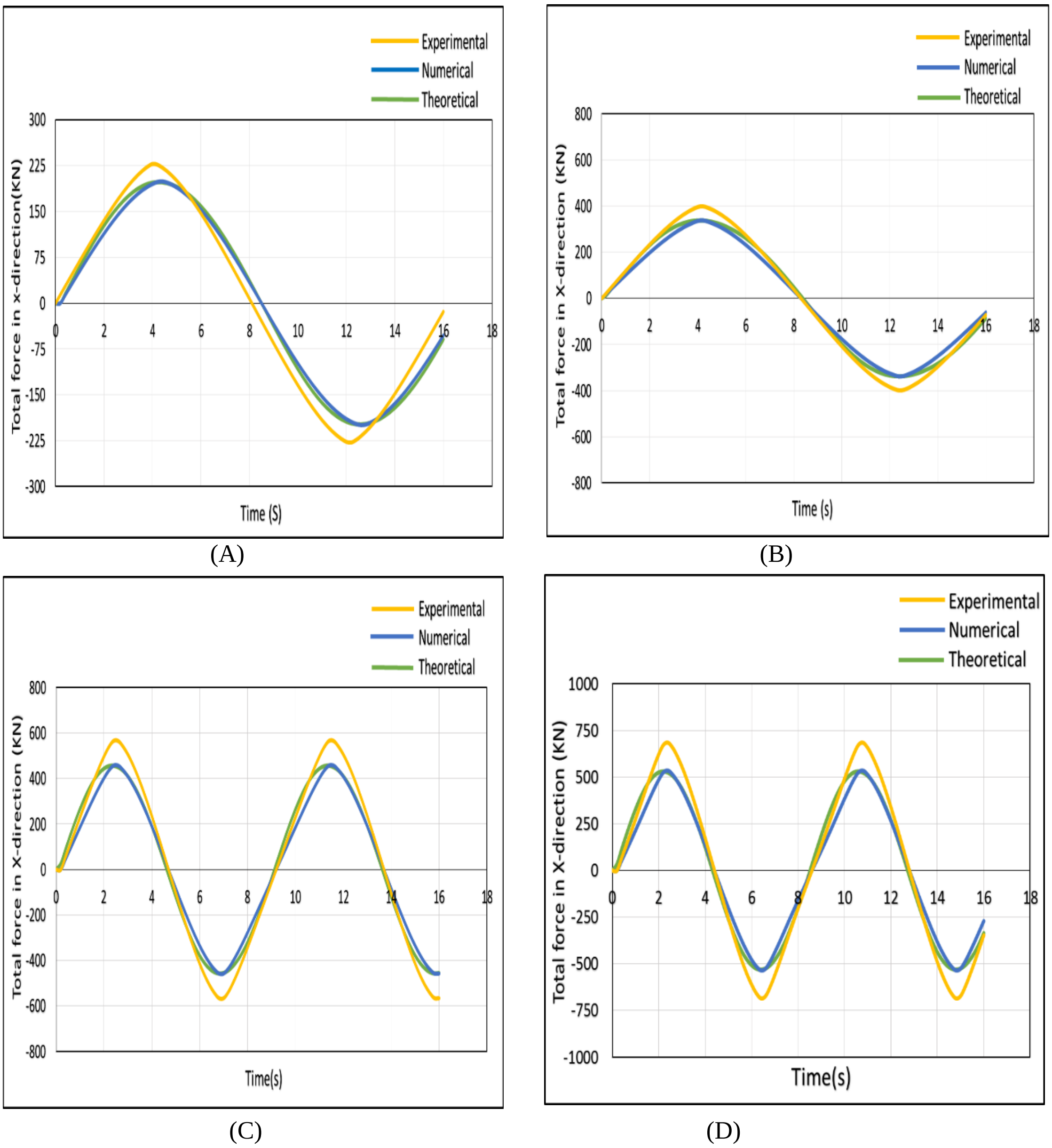

Figures (13): The results of total force for four cases (A, B, C and D) in X-direction.

There were a good agreement has been observed between theoretical and numerical results. But there is a deviation with experimental data, see table (3). The differences which was recorded in experimental part it was for several reasons such as: the small size of wave flume, even with the existence of waveabsorber at opposite side of wave generator, the probability of wave reflection remains exists from that side and also from the other two opposite sides. The other reasons which was played a major role in influence on recorded readings of wave forces is the vibration which was resulted from the movement of the gate especially at high frequency and also the impacting waves on the surface of vertical cylinder, this will effect on the signal of force transducer and lead to rise the readings.

To analyze the results graphs of total force in (x-direction), it was shown that the wave height and wave frequency play a major role in the terms of influence on the loads. In first and second case the frequency of the wave was the same (0.0605HZ), but the wave height in the second case increased by (1.7) times, it was noted that the wave forces is also increased by (46.65%). Also, the four case has the same wave height with second case (4.25m), but the wave frequency in the four case was higher by (2.9) times, it was found that the wave force also increased by (42.97%).

Table (3): comparison results

NO.	Total force (KN)				
	Experimental	Theoretical	ANSYS	Error% with Theo.	Error% with ANSYS
Case I	227.67	198.11	199.34	14.92	14.21
Case II	398.81	337.44	339.55	18.18	17.45
Case III	565.86	457.02	457.44	23.81	23.7
Case IV	684.51	530.57	534.77	29.01	28

13. Conclusion

From this study, the following conclusion can be highlighted:

I- An experimental investigation on wave impact on a slender vertical monopile foundation has been carried out under different properties of waves, it was shown that the results in experimental part is higher from theoretical and numerical, one of the main reason is due to large conversion rate when convert the results from the model to the prototype.

II- Hydrodynamic force is proportional to water depth, it's found that the maximum value of wave force at the surface of water when (Z=0), and begins decrease gradually until reach to the minimum value at the bottom of foundation.

III- The wave force increase when one or both of wave height and wave frequency increase.

IV- Due the small amplitude of wave height for all cases and because the current effect not taken into consideration, it was shown that the inertia force was dominate on drag force.

V- From the simulations of wave loading on a vertical monopile foundation, it can be concluded that the ANSYS-AQWA option is able to produce results from the model tests with good accuracy, although the number of elements is less than the others options such as (CFD) option.

Conflicts of Interest

The author declares that they have no conflicts of interest.

14. References

[1] P. Cuéllar. "Pile foundations for offshore wind turbines: numerical and experimental investigations on the behavior under short-term and long-term cyclic loading" PHD thesis, 2011.

[2] Aliyu Baba. "Concept of Hydrodynamic Load Calculation on Fixed Jacket Offshore Structures-—An Overview of Vertically Mounted Cylinder." Vol.3, Issue 3, p.p:65-74, 2014.

[3] Wind Support Structures to Sea Levels and Wave Conditions" Applied Sciences,vol. 9, issue 9,p.p:1855, 2019.

[4] A. C. Mendens, J. A. Kolodziej and H. J. D. correia. "Numerical modelling of wave-current loading on offshore jacket structures", WIT Transactions on The Built Environment, vol. 71, p.p: 1743-3509,

[5] P. D. Roy and S. Ghosh, "Force on vertically submerged circular thin plate in shallow water due to oblique wave", Indian Journal of Marine Sciences, vol.38, issue 4, p.p:411-417, 2009.

[6] Min-Su Park, Youn-Ju Jeong, Young-Jun You, and Jeongsoo Kim. "Numerical Analysis of a Gravity Substructure for 5MW Offshore Wind Turbine" International Journal of Engineering and Technology, vol. 10, No. 1, 2018.

[7] Masoomi Mohammad. "Model development and load analysis of offshore wind turbine", MSc, University of Toledo, 2014.

[8] Jian, Y., Zhan, J., & Zhu, Q. "Short crested wave–current forces around a large vertical circular cylinder", European Journal of Mechanics-B/Fluids, vol.27, issue 3, p.p: 346-360, 2008.

[9] Lin, Y. H., Chen, J. F., & Lu, P. Y. " A CFD model for simulating wave run-ups and wave loads in case of different wind turbine foundations influenced by nonlinear waves" Ocean Engineering, vol.129, p.p: 428-440, 2017.

[10] Paulsen, B. T., Bredmose, H., Bingham, H. B., & Schløer, S. "Steep wave loads from irregular waves on an offshore wind turbine foundation: Computation and experiment" In ASME 2013 32nd

International Conference on Ocean, Offshore and Arctic Engineering. American Society of Mechanical Engineers Digital Collection, 2013.

[11] Aggarwal, A., Chella, M. A., Kamath, A., Bihs, H., & Arntsen, A. "Irregular wave forces on a large vertical circular cylinder" Energy Procedia, vol.94,p.p: 504-516, 2016.

[12] Aliyu Baba. "Concept of Hydrodynamic Load Calculation on Fixed Jacket Offshore Structures-—An Overview of Vertically Mounted Cylinder." Vol.3, Issue 3, p.p:65-74, 2014.

[13] Vorhoelter, H., Will, J., Schmitt, P., & Puder, D. "Wave Loads on Monopile Structures" In STG Jahrbuch (Accepted/In press), Vol. 111, 2018.

[14] Noorzaei, J., Bahrom, S. I., Jaafar, M. S., Thanoon, W. A. M., & Mohammad, S. "Simulation of wave and current forces on template offshore structures" Suranaree J Sci Technol, vol.12, issue 3, p.p:193-210, 2005.

[15] J. M. J**.** Journée, and W. W. Massie, "OFFSHORE HYDROMECHANICS" , 2001.

[16] Deo, M. C. "Waves and structures." Indian Institute of Technology, Bombay (2013).

[17] ANSYS, “Aqwa user’s manual,” ANSYS Inc, 2019.

[18] ANSYS, “Aqwa Theory manual,” ANSYS Inc, 2019.

[19] Wu, Y. C. "Waves generated by an inclined-plate wavegenerator" International journal for numerical methods in fluids, vol.8, issue0.7, p.p: 803-81 1, 1988.

التحقق من قو موجات المياه المؤثره على القاعده الاسطوانيه للتوربينات البحريه الثابته

حسن محمد علوان　　اسراء يحيى داوود　　سجاد جواد كاظم

قسم الهندسه الميكانيكيه الجامعه التكنلوجيا بغداد العراق

Keffaat@mail.ru　　Israayheaa@yahoo.com　　zzaa8899@gmail.com

الخلاصه:

ان حساب احمال التصميم المؤثره على هياكل التوربينات البحريه هي عمليه معقده. لذلك تم كتابه هذه الورقه البحثيه للدراسه والتحقق من تاثير الظروف البيئيه وبلخصوص موجات المياه على الاحمال الهيدروديناميكيه المؤثره على قواعد الهياكل البحريه الثابته. لهذا الغرض تم اختيار قاعده اسطوانيه الشكل لتوربين هوائي ذو قدره (5 ميغا وات) مصمم من قبل المختبر الوطني للطاقه المتجدده في الولايات المتحده الامريكيه من اجل اجراء التجربه وحساب الاحمال الهيدروديناميكيه. تم اختبار هذه القاعده على عمق (25 متر). ابعاد الاسطوانه وعمق المياه بلاضافه لخواص موجات المياه تم تحويلها من الابعاد الحقيقيه الى الابعاد النموذجيه عن طريق علاقات فرود مع نسبه قياس (1:100). الموجات التي تم اختبارها هي موجات منتظمه وغير منكسره وذات بعدين فقط. بلنسبه للجانب النظري من هذه التجربه فان معادله موريسون لحاله عدم الحيود تعتبر اختيار مناسب لحساب الاحمال المؤثره على القاعده البحريه. تم برمجه هذه المعادله بواسطه لغه (C ++). هذه المعادله تتكون من جزئين: الجزء الاول يمثل قوة القصور الذاتي المرتبطه بتعجيل جزيء الموجه اما الجزء الثاني فهو قوه الاعاقه المرتبطه بسرعه جزيء الموجه. ($,C_D C_M$) هي معاملات خاصه بمعادله موريسون لكل من قوة القصور الذاتي وقوة الاعاقه على التوالي. هذه المعاملات يتم حسابها بطرق مختلفه بناءا على تجارب عمليه لكن القيم التي تم اعتمادها في هذه التجربه ماخوذه من مخططات خاصه بمعهد البترول الامريكي. من اجل حساب سرعه جزيء الموجه وكذلك التعجيل فان نظريه الموجه الخطيه الموضوعه من قبل العالم ايري تعتبر مناسبه للموجات المنتظمه وذات الارتفاعات القليله. من الناحيه العدديه فان محاكاة الامواج وكذلك حساب القوى تم باستخدام برنامج الانسزز وتحديدا خيار الاكوا نسخه (2019). من خلال النتائج التي تم الحصول عليها نستنتج ان قوة الامواج ترتبط بصوره مباشره بارتفاع وتردد الامواج حيث انها تزداد او تقل بازدياد احدهما او كليهما.

الكلمات الداله: نظريه ايري، للموجات القاعده الاسطوانيه التوربينات البحريه انسزز اكوا قوة الاعاقه قوة عزم القصور الذاتي.